Analysis of p-Cycle Capacity in WDM Networks

Dominic A. Schupke*

December 20, 2005

Abstract

The concept of p-cycles provides many characteristics, which are benficial for deployment and operation in WDM networks. We present a detailed analysis of the resource efficiency addressing several issues, which are essential to WDM networks. This includes novel investigations about the influence of the length of working paths and a detailed redundancy comparison of p-cycles with prevalent protection mechanisms.

In addition, we find several trends in the optimal p-cycle network design. One is the capacity smoothing effect that can be related to analytical capacity bounds. We can also identify that shorter p-cycles can facilitate optimal design in demand hot-spot regions.

Finally, we propose a novel concept of p-paths, which, when used additionally in a p-cycle design, is able to improve capacity efficieny. This concept is also interesting in terms of both theoretical bounding conditions and practical deployment.

Keywords: Protection, p-Cycles, Network Design, WDM Networks.

1 Introduction

Optical networks require recovery mechanisms, which use network resources efficiently, achieve fast recovery times, and are feasible in operation and management. It emerges

*The author is with Siemens, Corporate Technology, Information and Communications, Optical Networks and Transmission, Otto-Hahn-Ring 6, 81730 Munich, Germany. Tel: +49 89 636-43518, Fax: -51115. Email: dominic.schupke@siemens.com. This work is part of the work while the author was with the Institute of Communication Networks at Technische Universität München, Munich, Germany.

that the link-recovery mechanism concept of preconfigured protection cycles, or "p-cycles" for short, can meet these requirements [1, 2].

This paper comprises a detailed analysis on the resource efficiency, which is typically expressed in capacity or cost. While many research works have already indicated the p-cycles' resource efficiency, we pursue further analysis differing from existing literature (summarized below). In particular, we address the physical length of working paths, which is an important parameter for WDM networks and which influences the capacity efficiency. We also relate design results to theoretical results by finding a capacity smoothing effect. In addition, we propose the novel and attractive concept of p-paths, which are substructures of p-cycles. This paper builds upon the study in the previous conference contribution [3] and aims to provide a comprehensive presentation of the topic.

The first paper on p-cycles [1] by Grover and Stamatelakis considers models for the optimal design of p-cycle networks with 100% restorability. Five test network designs show that no or little additional capacity ("excess sparing") is needed in relation to a network with link-restoration. Reference [4] proves for fully meshed graphs with sufficient working and spare capacity that a preconfigured link protection mechanism can protect at best $(N-2)$ working links for every spare capacity unit consumed (N is here the number of nodes on the preconfiguration pattern). This limit is reached by p-cycles, but not by trees. The authors also show that, under the above assumptions, the redundancy of p-cycle networks is $1/(\overline{d}-1)$ with the number of p-cycle nodes tending to the number of network nodes ($\overline{d}$ is the average nodal degree in the network). Technical report [5] indicates that p-cycles are efficient from the structural point-of-view. In the study, a genetic algorithm can form arbitrary preconfigured protection patterns to optimize the network protection capacity. In the results, many optimal patterns resemble cyclic patterns, then called p-cycles, giving rise to use only these cycles as patterns for the optimization.

Grover and Doucette [6] compare results of non-joint optimization and joint optimization, and show that the joint design is much better in capacity than the non-joint design. The book by Grover [7] embraces much of the work on p-cycles summarzed so far. In the book, also Hamiltonian p-cycles are described. Hamiltonian p-cycles are the basis for presenting lower capacity bounds and the concept of semi-homogeneous p-cycle networks, in which every link carries a working capacity of w, except for selected links (protected as straddling links), which can carry w or $2w$.

Lipes [8] investigates electrically switched optical networks with dedicated and shared protection and optically switched networks with dedicated and p-cycle protection. In all

cases, the grooming function is electrical. Optically switched networks deploy optionally transponders. The author shows for a nine-node network that the p-cycle approach has significantly less total cost than the other architectures. This is mainly due to sparing in o-e-o conversions, since p-cycles realize shorter working paths and since the transponders for protection paths serve a double purpose, accessing p-cycles and regenerating the signal.

For single link failure scenarios, Rajan and Atamtürk [9] compare optimization results obtained by a joint formulation for unidirectional p-cycles, by an entire reconfiguration of the network, and by non-joint p-cycle optimization. In the results, the capacity efficiency of the joint optimization comes close to the one of reconfiguration, whereas a larger gap in efficiency resides between joint and non-joint optimization.

In [10], Birkan et al. present integer linear programs for joint optimization of static p-cycles including network equipment. For the eligible cycle set, the authors generate the k-shortest node-disjoint cycles, which do not contain links that cross. Compared with designs of networks without protection, p-cycles require 87-94% additional cost in test cases. Note that the test cases do not seem to allow low cost levels, since even shared path protection could outperform this only by a value of 73%. The study also investigates robust design for a given uncertainty of the demand. A set of demand matrices which occur with a given probability are given and the design aims to minimize a regret function. The regret function represents the tradeoff between the equipment cost of the design and the demand that is not carried because of lack of capacity in the design. The main intend of the authors is to motivate the employment of ILPs in the design of WDM networks. At the expense of optimality, they suggest to calculate with an allowed optimality gap of 5% reducing the computation times by a factor exceeding 1800 in many cases.

Mauz [11] investigates the joint p-cycle design problem for WDM networks with full wavelength conversion using an ILP, and no wavelength conversion using a heuristic. As in [3], the designs are based on unidirectional p-cycles. The paper proposes as heuristic approach for networks without wavelength conversion, a first-fit method to assign the wavelengths and p-cycles to working paths. For sample networks designed by the two approaches, networks without conversion require 40-60% more capacity than networks with full conversion. In [12], Mauz investigates the capacity of p-cycles using ILP and the joint approach. A case study results in redundancy values of 0.6, 0.7, and 1.3 for three hypothetical European networks with degree 4.3, 3, and 2.4, respectively.

Reference [3] investigates the deployment of p-cycles in WDM networks with and without wavelength conversion. The authors develop optimization models for the configuration

of the cycles and apply these on a case study for a pan-European network. The results in particular for wavelength converting networks show that p-cycles achieve high efficiency. A special consideration is the dependency on the allowed maximum physical p-cycle length. Unlike this paper, in [3] unidirectional p-cycles are used.

Reference [13] elaborates on the configuration of p-cycles in WDM networks with limited wavelength conversion. A major finding is that the total number of converters required for the network as a whole can be greatly reduced, with only a small increase in protection capacity.

This paper is structured as follows. Section 2 describes the protection principle of p-cycles. Section 3 contains the mathematical optimization model for p-cycle network design. Section 4 details several redundancy measures for the assessment of resource efficiency. Representative case study networks are summarized in Section 5. Sections 6 and 7 discuss numerical results regarding the length of working paths and of p-cycles, respectively. Section 8 presents the concept of "p-paths." Section 9 concludes the paper.

2 Protection Principle

We can regard p-cycles as a link-recovery mechanism. It is particularly interesting for optical networks, since link failures are the most frequent failure events in these networks.

We assume a network in which connections are switched individually (e.g., a WDM network with protection-switching on the optical channel level). Figure 1 depicts the protection principle of p-cycles for link protection. The p-cycle in Figure 1(a) is preconfigured as a closed connection on the cycle B-C-D-F-E-B. Preconfiguration means that the configuration is done before a failure occurs.

The p-cycle is able to protect working capacity on its own links, called *on-cycle* links, as shown in Figure 1(b). Upon failure of on-cycle link B-C, the p-cycle offers protection by the route on the remainder of the cycle (C-D-F-E-B). The protectable capacity on on-cycle links is thus one capacity unit. The protection of on-cycle links is logically equal to multiplex-section shared protection rings (MS-SPRings) in SDH and bidirectional line-switched rings (BLSRs) in SONET [14]. Unlike these rings, however, p-cycles also protect links outside the p-cycle path: Each link that has both its end points on the p-cycle can also be protected. Figure 1(c) shows the protection of such a link (E-D), which is called *straddling* link. We can provide two protection routes for straddling links, in the example, routes E-B-C-D and E-F-D. In effect, we can protect two working capacity units

of straddling links.

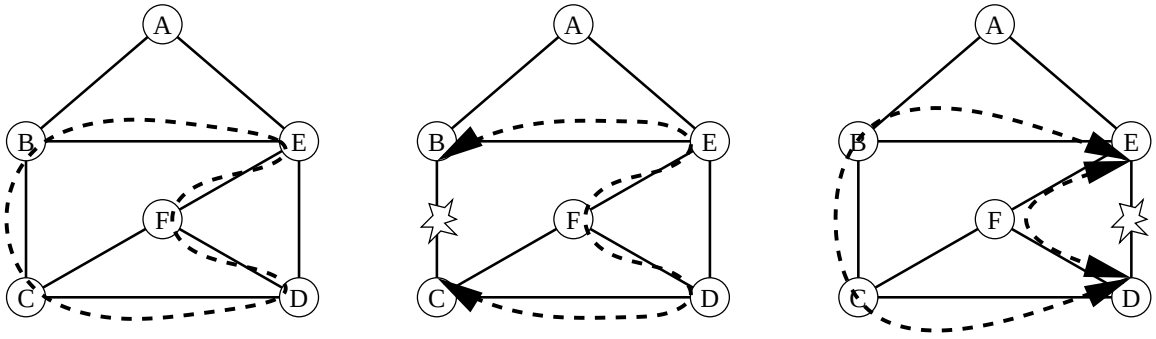

(a) A p-cycle (dashed line) in a network. (b) Protection of an on-cycle link. (c) Protection of a straddling link.

Figure 1: Protection principle of p-cycles for link protection.

Since the nodes adjacent to the failure perform protection switching, fast recovery times are possible. By analogy to automatic protection switching of SONET/SDH rings, we can assume recovery times of 50 ms.

3 Joint Optimization Model for p-Cycle Selection

We review the basic mathematical optimization model for the capacity-optimal selection of both working connections and link-protecting p-cycles. This model is called "joint" optimization model [6, 15, 11]. The other alternative is the "non-joint" optimization model, where working connections are routed first and the resulting working capacity on the links is given as fixed input for the optimal p-cycle selection [1, 2, 3].

The network to be protected is modeled by graph $G = (V, E)$. Associated with the graph are edge costs $z_e, \forall e \in E$, working capacities $w_e, \forall e \in E$, and protection capacities $p_e, \forall e \in E$.

Based on (precomputed) cycles with index-set C, the two matrices $\mathbf{\Pi}$ and $\mathbf{\Phi}$ of size $(|E|, |C|)$ are given. An matrix entry $\pi_{e,k} \in \{0, 1\}$ of $\mathbf{\Pi}$ indicates whether edge $e \in E$ is element of cycle k. The matrix entry $\phi_{e,k} \in \{0, 1, 2\}$ of $\mathbf{\Phi}$ indicates how many working capacity units on edge $e \in E$ are protectable by a p-cycle unit on cycle $k \in C$. These latter matrix entries correspond to the useful paths, as denoted in [1], i.e., the number of useful paths a p-cycle can offer for protection of the edge.

At this point we also define the straddling link matrix $\mathbf{\Sigma} = \frac{1}{2}(\mathbf{\Phi} - \mathbf{\Pi})$. A matrix entry $\sigma_{e,k} \in \{0,1\}$ of $\mathbf{\Sigma}$ indicates whether edge $e \in E$ is a straddling link of cycle $k \in C$ (i.e., has a "straddling relationship" to the cycle [2]) or not. A column of the matrix $\mathbf{\Pi} + \mathbf{\Sigma} = \mathbf{\Phi} - \mathbf{\Sigma}$ in effect indicates which edges can be protected by the corresponding cycle, without quantifying how much capacity can be protected on each edge.

For the p-cycles configuration, we are interested in the number of p-cycle units n_k for each cycle $k \in C$ that is needed, i.e., the cycle capacity on cycle k.

For joint optimization, we additionally have to model working capacity computation. For a path-flow formulation, we are given a set of demand pairs $D \subset V \times V$, and for each demand pair $\delta \in D$ the number of demands d_δ, an index-set of eligible working paths Q_δ, and indicators $\gamma_{e,q} \in \{0,1\}$ being one if working path $q \in Q_\delta$ is on link $e \in E$, zero otherwise. Additional solution variables are the demand flow variables $f_{\delta,q}$.

We state the problem for joint optimization as follows:

$$\min \quad \sum_{e \in E} z_e(w_e + p_e) \tag{1}$$

$$p_e = \sum_{k \in C} \pi_{e,k} n_k, \ \forall e \in E \tag{2}$$

$$w_e \leq \sum_{k \in C} \phi_{e,k} n_k, \ \forall e \in E \tag{3}$$

$$w_e = \sum_{\delta \in D} \sum_{q \in Q_\delta} \gamma_{e,q} f_{\delta,q}, \ \forall e \in E \tag{4}$$

$$d_\delta = \sum_{q \in Q_\delta} f_{\delta,q}, \ \forall \delta \in D \tag{5}$$

$$p_e \in [0, \infty), \ \forall e \in E \tag{6}$$

$$w_e \in [0, \infty), \ \forall e \in E \tag{7}$$

$$f_{\delta,q} \in \{0,1,2,\ldots\}, \ \forall \delta \in D, q \in Q_\delta \tag{8}$$

$$n_k \in \{0,1,2,\ldots\}, \ \forall k \in C \tag{9}$$

The Objective (1) minimizes the cost-weighted total capacity. Constraints (2) determine the protection capacity allocation, and Constraints (3) ensure the working capacity to be protected. Note that the right-hand side of (3) is the protect*able* capacity, which can be larger than the working capacity. Constraints (4) determine a link's working capacity by the sub-flows of all demands on the link. For a demand pair, Constraints (5) equate the demand to its individual sub-flows on the given paths. The working and protection capacity variables, which are auxiliary variables here, are defined in (6) and (7), respec-

tively. The integer flows (which can be upper bounded by their demands) are defined in (8) and the integer p-cycle units are defined in (9).

The joint optimization problem has $2|E|$ continuous variables, $(|C| + \sum_{\delta \in D} |Q_\delta|)$ integer variables, and $(3|E| + |D|)$ constraints. Using variable substitution of (2) in (1) and (4) in (3), the continuous variables are dropped and the number of constraints reduces to $(|E| + |D|)$.

4 Network Redundancy

To normalize capacity and cost values, we define several redundancy measures [7] and derive a simple bound on the logical redundancy.

We define the *logical redundancy* (r), or simply *redundancy*, as the ratio of the protection capacity to the working capacity. The *cost-weighted redundancy* (r_c) is the ratio of the cost-weighted protection capacity to the cost-weighted working capacity, where the weights are given cost-values per link. Consider an optimal working capacity design, yielding the minimum possible working capacity, and denote the difference between the working capacity of any other design and this capacity as additional working capacity. The *standard redundancy* (r_s) is the ratio of the sum of the protection capacity and the additional working capacity to the minimum possible working capacity. With an analogous weighting to cost-weighted redundancy, we define the *cost-weighted standard redundancy* (r_{cs}).

A lower bound on the logical redundancy of link-recovery in networks with homogeneous capacity can be derived as follows. After failure of physical link $i \in E$ in Figure 2, the surviving links have to provide enough protection capacity to carry the working capacity

$$w_i \leq \sum_{\substack{j \in E_m \\ i \neq j}} p_j = -p_i + \sum_{j \in E_m} p_j, \ \forall i \in E_m, m \in V \tag{10}$$

where E_m is the set of edges incident to node $m \in V$.

For homogeneous link capacity $w_i + p_i = c, \forall i \in E$ holds (note that we do not have any further spare capacity). We simplify Relation (10) into

$$c \leq \sum_{j \in E_m} p_j, \ \forall m \in V. \tag{11}$$

Formula (11) says, that the protection capacity node m "sees" is at least as high as the

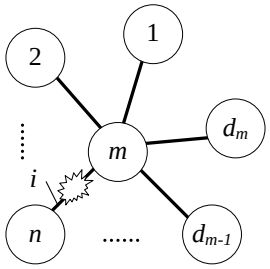

Figure 2: A node m with the set of incident links E_m connecting the d_m adjacent nodes and the failure of some incident link i.

capacity of one link. Therefore, in the optimal case, every node sees the same protection capacity, independently of its degree.

Summing Inequality (11) over all nodes yields

$$|V|c \leq \sum_{m \in V} \sum_{j \in E_m} p_j = 2 \sum_{e \in E} p_e. \tag{12}$$

With $|E|c = \sum_{e \in E} (w_e + p_e)$ and the average nodal degree $\overline{d} = \frac{2|E|}{|V|}$, we find the bound on the logical redundancy

$$r = \frac{\sum_{e \in E} p_e}{\sum_{e \in E} w_e} \geq \frac{1}{\overline{d} - 1}. \tag{13}$$

5 Case Study Networks

We investigate several properties of p-cycles with a focus on networks having full wavelength conversion. Reference [13] shows that we can treat a WDM network with appropriate partial wavelength conversion as a network with full wavelength conversion. In other words, we are able to achieve the results for networks without wavelength continuity constraints by general WDM networks if we deploy a moderate degree of conversion in the network. Furthermore, today's networks, based on point-to-point WDM systems terminated by o-e-o conversion [14], are more likely to migrate to networks with full wavelength conversion first, and in future, technology advances in wavelength conversion and regeneration (e.g., optical wavelength conversion [14] and optical regeneration working on multiple channels) could make these networks even cost-effective. Conversely, restrictions that hold for full converting networks also hold for networks with no or some wavelength conversion.

We study four simple (no self-loops and no parallel links) and two-node-connected

Table 1: Characteristic parameters of the case study networks.

	eur_net239	eur_net266	ger_net	nsf_net
Number of nodes $\|V\|$	11	28	17	14
Number of links $\|E\|$	26	41	26	21
Average nodal degree $\overline{d}$	4.73	2.93	3.06	3.00
Sum of physical link lengths (in km)	15045	25640	4427	27280
Longest shortest path in physical length (in km)	1660	5051	951	5316
Number of (simple) cycles $\|C\|$	3531	1469	135	139
Average hop cycle length	8.75	16.35	9.78	9.59
Maximum hop cycle length	11	27	17	14
Total demand $\sum_{\delta \in D} d_\delta$	176	1008	1021	2710

physical networks. The `eur_net239` network is based on the pan-European network as used in the COST Action 239 [16]. In order to derive bidirectional lightpath granularity from the demand matrix in [16], we adapt two unsymmetrical demand pairs by taking the higher value and divide the values for the given demand transmission rates by 2.5 Gbit/s. The next three networks are the optical transport network reference scenarios as suggested in [17]. The `eur_net266` network is based on the "basic reference topology (BT) for a pan-European fibre-optic network" as defined in the COST Action 266 [18]. The `ger_net` network is based on a hypothetical national backbone network as used, for instance, in [19]. The `nsf_net` network is based on the National Science Foundation Network (NSFNET) used, for instance, in [20]. Table 1 lists several parameters of the networks.

We optimize using the model in Section 3 and CPLEX [21]. The demand of the networks is scaled by 10 and the objective is physical length based, i.e., $z_e = l_e$ where l_e denotes the length of the physical link $e \in E$.

6 Dependency on the Length of Working Paths

We discuss optimization results for the networks with special respect to the physical length of the working paths. We start with an analysis of the different redundancies, relate several capacity smoothing effects to the theoretical results of Section 4, and end with a closer look at the length characteristics of working paths.

We analyze the dependency on the length of working paths by varying the maximum allowed relative deviation from the shortest paths. We denote this deviation β. In other words, we allow paths for a demand pair to be at most $(1 + \beta)$ times longer than the

shortest possible path. We add these substitutable constraints to the problem

$$f_{\delta,q} = 0,\ \forall \delta \in D, q \in Q_\delta : l_{\delta,q} > (1+\beta) \min_{a \in Q_\delta} l_{\delta,a} \tag{14}$$

where $l_{\delta,a}$ denotes the physical length of a path with indices $\delta \in D$ and $a \in Q_\delta$. By setting $\beta = 0$, we obtain the non-joint optimization problem based on working capacity obtained by shortest path routing, if all the shortest paths are unique. This holds for all our networks except for `eur_net239`, for which the results are, however, comparable if some shortest path is chosen.

6.1 Redundancy Analysis

Figures 3 to 4 show redundancy values for the networks `eur_net239` and `eur_net266` under different designs. The results for `ger_net` and `nsf_net` are similar in characteristic to the ones of `eur_net266`.

The figures depict designs for p-cycles in comparison with designs for virtual rings and dedicated path protection, the most prevalent recovery mechanism concepts in optical networks. The ring designs are optimized in the same manner as for p-cycles. However, as straddling links cannot protect working capacity, we substitute the entries of $\mathbf{\Phi}$ for the entries of $\mathbf{\Pi}$ in Constraints (3) and use the such modified joint optimization model (β also applies). The dedicated path protection designs reserve two link-disjoint paths for a demand unit and minimize the sum of all path-lengths (path length restrictions do not apply).

The cost-weighted standard redundancy r_{cs} makes a fair comparison between the designs possible. The figures include the (non-cost-weighted) redundancy r and the cost-weighted redundancy r_c for p-cycles, and the degree-based bound $1/(\overline{d}-1)$.

In all four cases, p-cycles significantly outperform the two other designs in the cost-weighted redundancy. While dedicated path protection and rings do not fall below 130% and 100% cost-weighted redundancy, respectively, p-cycles can achieve as little as 38% cost-weighted redundancy (`eur_net239`).

In all redundancy measures, p-cycles achieve values below 40% in the `eur_net239` whereas the values stay (partially significantly) above 50% in the other networks. We can explain this by the difference in the (logical) redundancy r in conjunction with the $1/(\overline{d}-1)$ bound. Although (as derived in Section 4) the bound is only applicable if we can make the homogeneity assumption, we can use it as an estimation of what (non-cost-weighted)

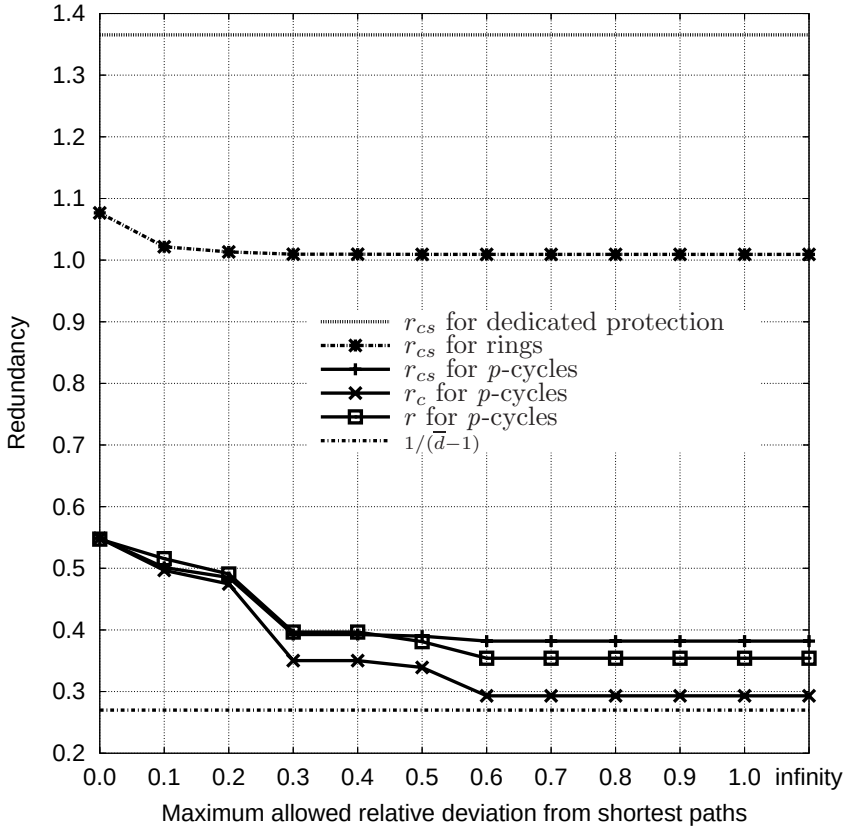

Figure 3: Redundancy measures over deviation β for the `eur_net239`.

redundancy we can reach at best (see also the capacity smoothing discussion below). We calculate the degree-based bound as 27% for `eur_net239` while the bound is at least 50% for the other networks. This supports that in networks with high nodal degrees, we can choose from many protection path alternatives, and thus, are able to implement more efficient p-cycle designs than in networks with low nodal degrees. Note that the logical redundancy for rings and dedicated path protection cannot fall below 100%.

It becomes apparent that the longer the paths are allowed to be, the better the results are. As we allow more paths (i.e., longer paths), the optimization can choose from more possibilities and, thus, is able to reach better results. The opposite aim is to keep paths short, e.g., because of signal degradation effects [14]. Therefore, in the figures, we can find a compromise between the contradicting aims. If, say, we allow $\beta = 0.5$, the cost-weighted redundancy of all networks is close to the best case ($\beta \to \infty$). In the step from $\beta = 0$ (equivalent non-joint design) to $\beta = 0.2$, which means a deviation of only 20%, p-cycles

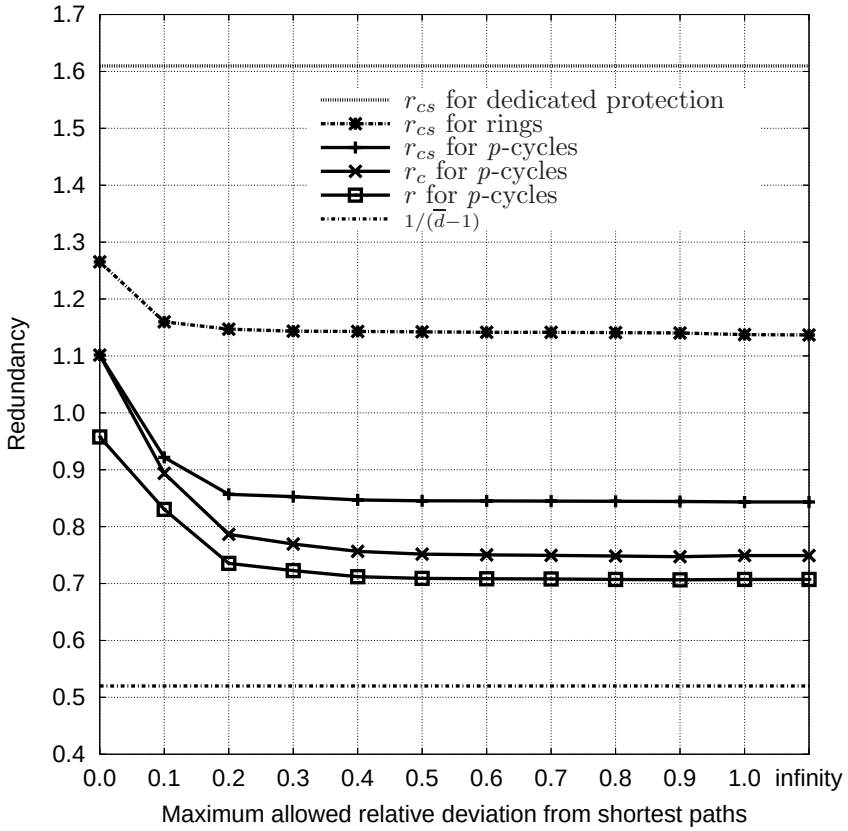

Figure 4: Redundancy measures over deviation β for the `eur_net266`.

are already able to improve cost-weighted redundancy significantly (in all cases except for `eur_net239`, it drops from a value over 110% to a value below 87%). We elaborate on the chosen paths lengths below.

Another approach to decrease redundancy is to use a routing method that differs from shortest path routing and that is more suited to p-cycles. Reference [3] shows, for instance, that routing that balances the load on the links is beneficial to reduce p-cycle redundancy. In the same interpretation as above, by giving up shortest paths, which means we give up optimal *working* capacity, we are able to achieve better efficiency by this balancing routing, and, thus, we approach optimal *total* capacity.

6.2 Capacity Smoothing

In the following, we show a capacity smoothing effect: The designs tend to realize homogeneous link capacity, for which the redundancy bound $1/(\overline{d}-1)$ applies (Section 4).

Figure 5 depicts three different normalized capacity measures, which are related to (11). The first measure is the normalized standard deviation of the link capacity

$$\sigma_c = \frac{\frac{1}{|E|}\sqrt{|E| \sum\limits_{e\in E}(w_e+p_e)^2 - (\sum\limits_{e\in E}(w_e+p_e))^2}}{\frac{1}{|E|}\sum\limits_{e\in E}(w_e+p_e)}. \tag{15}$$

It measures how widely the link capacities are dispersed relatively from the average link capacity value. This value is zero for a true homogeneous link capacity network.

The second measure is the normalized standard deviation of the protection capacity on links incident at nodes

$\sigma_p =$

$$\frac{\frac{1}{|V|}\sqrt{|V| \sum\limits_{m\in V}(\sum\limits_{(m,n)\in E} p_{(m,n)})^2 - (\sum\limits_{m\in V}\sum\limits_{(m,n)\in E} p_{(m,n)})^2}}{\frac{1}{|V|}\sum\limits_{m\in V}\sum\limits_{(m,n)\in E} p_{(m,n)}}. \tag{16}$$

This measure relates to the right-hand side of Inequality (11), i.e., it quantifies how close we are to the situation that every nodes sees the same protection capacity (independently of the degree).

The third measure is the average nodal protection capacity to the average link capacity ratio

$$\rho_{pc} = \frac{\frac{1}{|V|}\sum\limits_{m\in V}\sum\limits_{(m,n)\in E} p_{(m,n)}}{\frac{1}{|E|}\sum\limits_{e\in E}(w_e+p_e)}. \tag{17}$$

We can associate the numerator with the left-hand side of Inequality (11), i.e., it is the average protection capacity a nodes sees. The denominator determines the average link capacity and represents the left-hand side of Inequality (11). If the ratio ρ_{pc} becomes closer to one and σ_c in Expression (15) becomes closer to zero, Inequality (11), the homogeneous link capacity inequality, becomes tighter.

Figure 5 shows the three measures σ_c, σ_p, and ρ_{pc} for the `eur_net239` design series from above. Since the characteristics for the three other study networks are similar, we only show the `eur_net239` results.

The more we increase β, i.e., the more the optimization is able to route working paths as needed, the lower all the measures tend to be. The decrease of the link capacity deviation σ_c and the decrease of the node-related protection capacity deviation σ_p indicate link capacity smoothing. Therefore, the optimization aims at lowering the dispersion of these values, and thus, it approaches a homogeneous link capacity network design. Also the gap between nodal protection capacity and link capacity becomes smaller (ρ_{pc}-curves).

Hence, we can conclude that an optimal p-cycle design aims to reach the homogeneous link capacity case. This is supported by the affinity to form large cycles (see below). In fact, since for any link the sum of Constraints (2) and (4) is the same using Hamiltonian p-cycles, networks deploying only Hamiltonian p-cycles are homogeneous in link capacity.

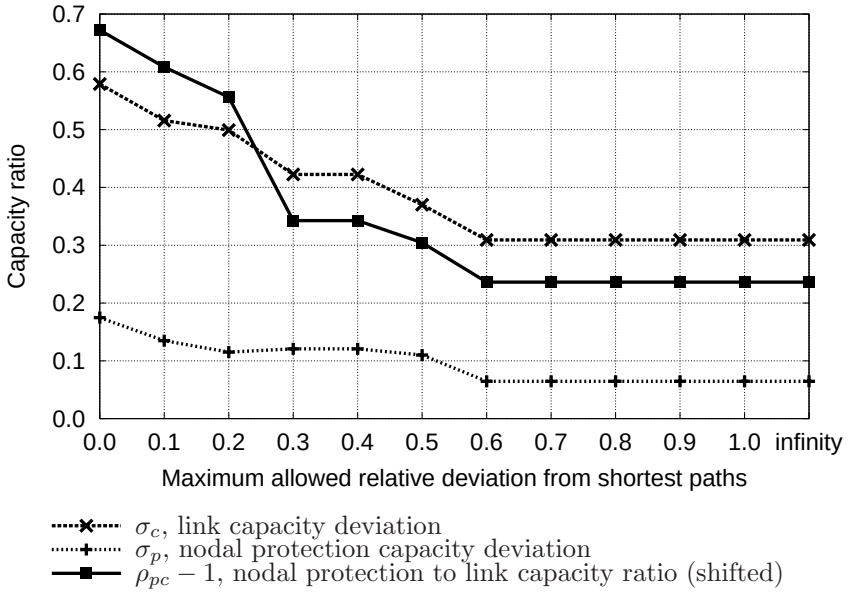

Figure 5: Normalized capacity measures over deviation β for the `eur_net239`.

Note that a *working capacity* smoothing effect has been found for general link-restoration schemes in [7], where also joint optimization chose load-leveling on working paths without any extreme deviation from the shortest paths.

6.3 Analysis of the Length of Working Paths

Figure 6 presents for the `eur_net239` what relative deviation from the shortest paths and from the hop-minimal paths is on average present in the optimal results. The figure also

shows the bounding value for the average relative deviation from shortest paths (bisector). Again, the characteristics for the three other study networks are similar.

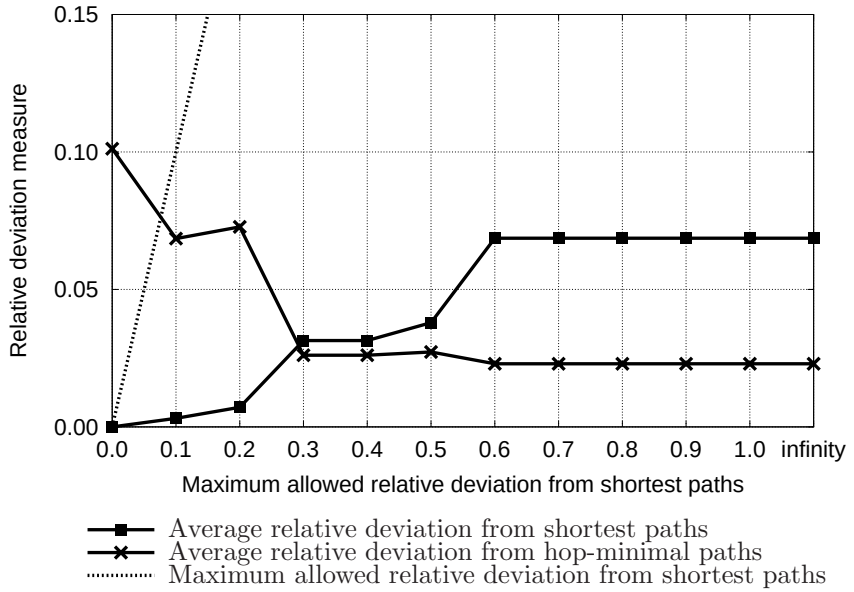

Figure 6: Length deviation of working paths over deviation β for the `eur_net239`.

We calculate the average relative deviation from shortest paths by

$$\frac{1}{\sum\limits_{\delta\in D} d_\delta} \sum_{\delta\in D} \sum_{q\in Q_\delta} f_{\delta,q} \frac{l_{\delta,q}}{\min\limits_{a\in Q_\delta} l_{\delta,a}} \tag{18}$$

and the average relative deviation from the minimal-hop paths by

$$\frac{1}{\sum\limits_{\delta\in D} d_\delta} \sum_{\delta\in D} \sum_{q\in Q_\delta} f_{\delta,q} \frac{h_{\delta,q}}{\min\limits_{a\in Q_\delta} h_{\delta,a}} \tag{19}$$

where $h_{\delta,a}$ denotes the hop length of a path with indices $\delta \in D$ and $a \in Q_\delta$.

The results show that the paths are on average at most 10% longer in physical length than the shortest paths. As the average relative deviation from shortest paths is significantly lower than the maximum allowed relative deviation from shortest paths (bisector), we conclude that only few paths require relaxation in physical length.

By increasing β, the average relative deviation from shortest paths increases monotonically while the average relative deviation from hop-minimal paths tends to decrease. We at-

tribute this to a substitution effect: The more hops physical paths need, the more capacity units p-cycles have to protect. Therefore, using working paths with slightly longer physical length but with less hops, the p-cycle capacity can decrease and the resulting total cost-weighted capacity can decrease, too.

7 p-Cycle Length Distribution

Figure 7 shows for all networks the hop-length distribution of the number of selected p-cycles in the optimal solution of the joint model ($\beta \to \infty$).

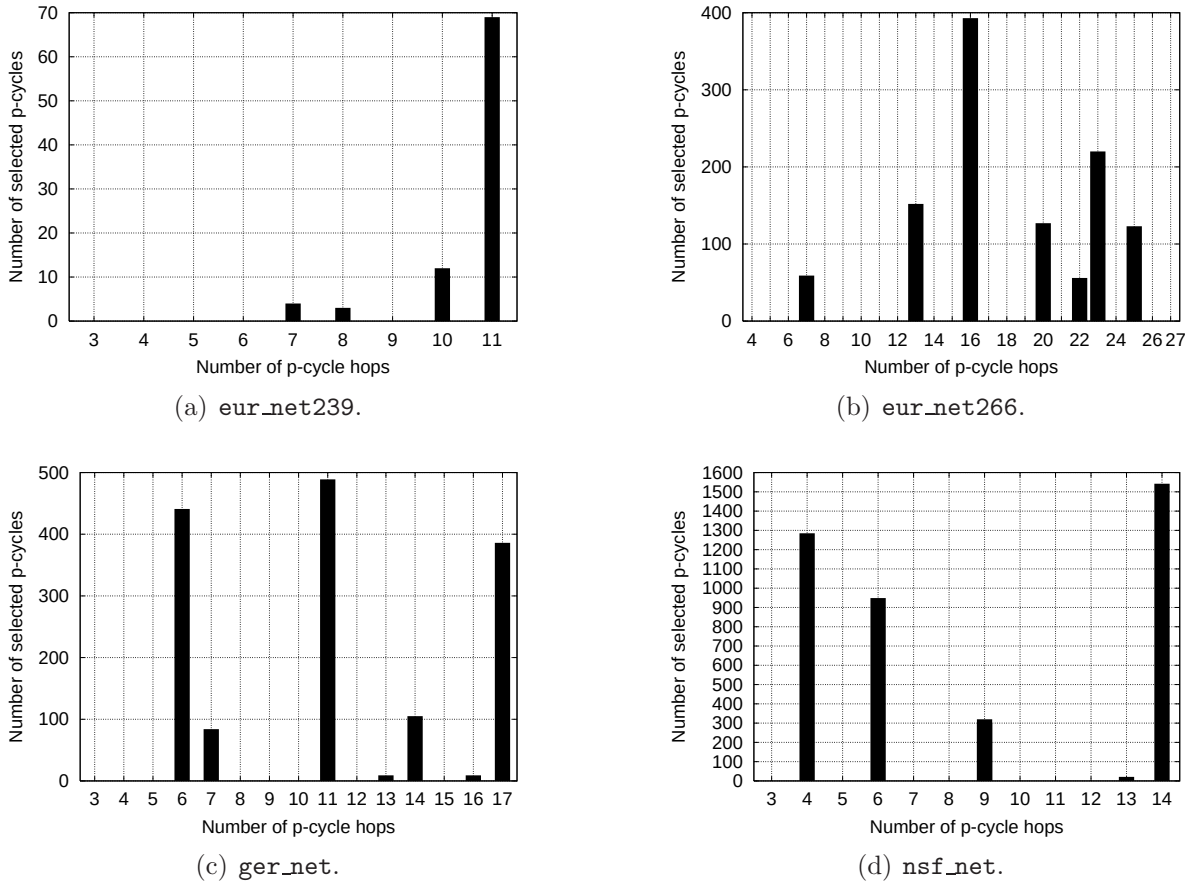

(a) `eur_net239`. (b) `eur_net266`.

(c) `ger_net`. (d) `nsf_net`.

Figure 7: p-Cycle hop-length distributions for deviation $\beta \to \infty$.

For all the networks, the optimal solution has a large amount of p-cycles with many hops. This is in accordance with [4], stating that "there should be a significant number

of large [...] p-cycles." In fact, all networks except for the `eur_net266` (which is not Hamiltonian) have a significant number of Hamiltonian p-cycles in the optimal solution.

For all networks excluding `eur_net239`, a considerable number of shorter p-cycles is present. p-Cycles with a low number of hops cannot cover as much working capacity as p-cycles with a larger number of hops. We can reason the choice for these cycles by high local traffic requirements ("demand hot-spots"). For each network, we can calculate the amount of demand between the nodes of the small cycles with high capacity. In the `eur_net266`, only one 16-hop cycle (which is already a longer cycle) accounts for the high p-cycle number in Figure 7(b). The demand between the nodes of the short cycles is 47% of the total demand. Therefore, dedicated p-cycles can cover this locally appearing traffic amount. Similar observations can be made for the two other networks. In the `ger_net`, the nodes of the 6-hop cycle and the 11-hop-cycle account for 16% and 45% of the demand, respectively. In the `nsf_net`, the nodes of the 4-hop cycle and the 6-hop-cycle account for 18% and 20% of the demand, respectively. The difference in the number of smaller p-cycles between `eur_net239` and the other networks can be attributed to the dependency on the connectivity. A well meshed network (as the `eur_net239`) can cover a number of nodes with few long p-cycles, whereas a sparsely meshed network (e.g., one of the other networks) requires for the same number of nodes many short p-cycles.

8 *p*-Cycles and *p*-Paths

In this section, we pursue a novel approach, which combines p-cycles with line segments. We can regard them as degenerated p-cycles. Similarly to the name "p-cycle," we call such protecting line segment preconfigured protection path or "p-path." A p-path is a path obtained by removal of one edge of a cycle. p-Paths differ from p-cycles in the protection capacity and the protectable working capacity.

Figure 8 depicts an example of a p-path B-C-D-A. As for p-cycles, the p-path has one protection capacity unit on its links. Unlike p-cycles, the p-path cannot protect these (on-path) links. The p-path can only protect working capacity on straddling links. As only one protection path is possible on the p-path, it can also protect only one working capacity unit per straddling link. We can construct the p-path by removing link A-B from p-cycle A-B-C-D-A. We call such a link "closure link."

p-Paths can be operated by a slightly modified p-cycle protection switching protocol. For correct operation, the protection paths for the straddling links have to be arbitrated

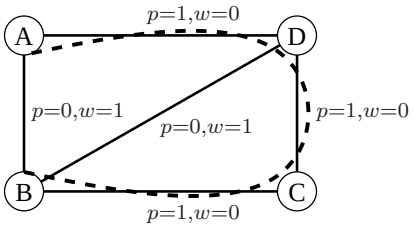

Figure 8: Example for a p-path.

to follow the p-path.

For the design, we extend the joint model by additional variables

$$\tilde{n}_{k,e'} \in \{0,1,2,\ldots\},\ \forall k \in C, e' \in E : \pi_{e',k} > 0 \tag{20}$$

and we substitute Constraints (2) and (3) for

$$p_e = \sum_{k \in C} \pi_{e,k} n_k + \sum_{k \in C} \sum_{e' \in E : \pi_{e',k} > 0} (\pi_{e,k} - \delta_{e',e}) \tilde{n}_{k,e}, \quad \forall e \in E \tag{21}$$

$$w_e \leq \sum_{k \in C} \phi_{e,k} n_k + \sum_{k \in C} \sum_{e' \in E : \pi_{e',k} > 0} (\sigma_{e,k} + \delta_{e',e}) \tilde{n}_{k,e}, \quad \forall e \in E \tag{22}$$

where $\delta_{e',e}$ indicates by $\delta_{e',e} = 1$ if $e' = e$ and zero otherwise.

We index the variables for the integer p-path units in (20) over the cycles and the closure links. In comparison with Constraints (2) and (3), we add the p-path protection capacity (as for p-cycles except for the closure links) in Constraints (21) and the p-path protectable capacity (straddling links and closure links) in Constraints (22). p-Paths require at most $|C||E|$ additional integer variables.

The overall optimization model outputs an optimal combination of p-cycles in Expression (9) and p-paths in Expression (20), where we obtain each path from a corresponing cycle by removing the cycle's closure link e' in Expression (20). We see the virtue of this approach for capacity-restricted networks, in which some links have little or no capacity

available for protection usage. An easy example is a congested link (exhausted by working capacity) in a chain of degree-two nodes of a network where the other links in the chain have no capacity to protect. While we may still find a line segment protecting this link, we cannot find a true p-cycle to protect it. It can also be beneficial for non-joint optimization, for which working paths cannot be adjusted such that p-cycles achieve highest efficiency.

In addition, we highlight that the p-cycle with p-path optimization can calculate a lower bound of the protection capacity an optimal p-cycle-only network truly needs, since there are two cases for which an optimal p-cycle does not need all its protection capacity. The first case is that a p-cycle protects only straddling links with one working capacity unit. Thus, we can spare the protection capacity which is needed by one of the straddling links' protection path alternatives. The second case is that a p-cycle protects additionally one working capacity unit on one of its on-cycle links. Thus, we can spare protection capacity on this protected link. As p-paths cover both cases, the p-cycle with p-path optimization is able to provide the bounding value.

For the four networks with unlimited capacity and a demand scaling of ten, we find that additional p-paths are able to lower the cost-weighted redundancy r_c only in the non-joint design. For the `eur_net266` and the `ger_net`, this redundancy reduces by 2% and 8%, respectively, otherwise it stays constant. To exemplify the capacity-restricted case, we limit the capacity of every link to 400 units in the `ger_net` and assume a demand scaling of one. In the non-joint design, no feasible solution is possible with only p-cycles. However, we obtain a solution using both p-cycles and p-paths.

9 Conclusions

We investigated link-recovery p-cycles within case studies for WDM networks with full or sufficient wavelength conversion. Using p-cycles is much more capacity efficient than using dedicated path protection or rings. The p-cycle redundancy significantly drops if working paths become slightly longer than the shortest paths. p-Cycle design tends to smooth link capacity to approach link capacity homogeneity in the network. An optimal set of p-cycles has a large portion of p-cycles with many hops, while at demand hot-spots shorter p-cycles come in place. The approach of p-paths is able to support p-cycles in capacity-restricted situations. p-Paths can be regarded as degenerated p-cycles, which avoid unused protection capacity that can be present in p-cycle-only networks.

The numerical results indicate that p-cycles seem to be particularly useful for WDM

networks in two main respects. Firstly, working paths can be kept short and still the best-case results are nearly attained, which can facilitate transmission engineering dealing with limitations due to signal degradation effects. Secondly, optimal p-cycle design tends to smooth capacity to achieve homogeneous capacity. In the short and mid term, we deal with WDM networks with single transmission systems per physical link. As transmission systems typically offer a fixed number of wavelength channels, we can regard WDM networks as homogeneous capacity networks. Hence, p-cycles are able to efficiently exploit this capacity and can avoid costly installation of parallel transmission systems.

Further work can consider the concept of p-paths in more detail. While the consideration of p-cycles in networks with dynamic traffic is also an important reseach topic, we note that the above results also apply for dynamic networks which use the concept of "protected working capacity envelope" [22].

References

[1] W. D. Grover and D. Stamatelakis, "Cycle-oriented Distributed Preconfiguration: Ring-like Speed with Mesh-like Capacity for Self-planning Network Restoration," in *Proceedings of the IEEE International Conference on Communications (ICC)*, (Atlanta, GA, USA), June 1998, vol. 1, pp. 537–543.

[2] W. D. Grover and D. Stamatelakis, "Bridging the ring-mesh dichotomy with p-cycles," in *Proceedings of the International Workshop on Design of Reliable Communication Networks (DRCN)*, (Munich, Germany), Apr. 2000, pp. 92–104, Invited Talk.

[3] D. A. Schupke, C. G. Gruber, and A. Autenrieth, "Optimal Configuration of p-Cycles in WDM Networks," in *Proceedings of the IEEE International Conference on Communications (ICC)*, (New York City, NY, USA), April–May 2002, vol. 5, pp. 2761–2765.

[4] D. Stamatelakis and W. D. Grover, "Theoretical Underpinnings for the Efficiency of Restorable Networks Using Preconfigured Cycles ("p-cycles")," *IEEE Transactions on Communications*, vol. 48, no. 8, pp. 1262–1265, Aug. 2000.

[5] D. Stamatelakis and W. D. Grover, "Network Restorability Design Using Preconfigured Trees, Cycles, and Mixtures of Pattern Types," Tech. Rep. TR-1999-05, TRLabs, (Edmonton, AB, Canada), Oct. 2000.

[6] W. D. Grover and J. E. Doucette, "Advances in Optical Network Design with p-Cycles: Joint optimization and pre-selection of candidate p-cycles," in *Proceedings of the IEEE/LEOS Summer Topical Meeting on All-Optical Networking*, (Mont Tremblant, QC, Canada), July 2002, pp. WA2–49–WA2–50.

[7] W. D. Grover, *Mesh-based Survivable Networks: Options and Strategies for Optical, MPLS, SONET and ATM Networking*, Prentice Hall, Upper Saddle River, 2003.

[8] L. Lipes, "Understanding the trade-offs associated with sharing protection," in *Proceedings of the IEEE/OSA Optical Fiber Communication Conference (OFC)*, (Anaheim, CA, USA), Mar. 2002, pp. 786–787.

[9] D. Rajan and A. Atamtürk, *Telecommunications Network Design and Management (Editors: G. Anandalingam and S. Raghavan)*, chapter Survivable Network Design: Routing of Flows and Slacks, pp. 65–81, Kluwer Academic Publishers, Boston, Dordrecht, London, 2003.

[10] G. Birkan, J. L. Kennington, E. V. Olinick, A. Ortynski, and G. Spiride, "Making a Case for Using Integer Programming to Design DWDM Networks," Tech. Rep. 02-EMIS-02, Southern Methodist University, School of Engineering, (Dallas, TX, USA), Sept. 2002, Also in Optical Networks Magazine, vol. 4, no. 6, November–December 2003.

[11] C. Mauz, "p-cycle Protection in Wavelength Routed Networks," in *Proceedings of the Working Conference on Optical Network Design and Modelling (ONDM)*, (Budapest, Hungary), Feb. 2003.

[12] C. Mauz, "Unified ILP Formulation of Protection in Mesh Networks," in *Proceedings of the International Conference on Telecommunications (ConTEL)/Workshop on All-Optical Networks (WAON)*, (Zagreb, Croatia), June 2003, vol. 2, pp. 737–741.

[13] D. A. Schupke, M. C. Scheffel, and W. D. Grover, "Configuration of p-Cycles in WDM Networks with Partial Wavelength Conversion," *Photonic Network Communications, Journal, Kluwer Academic Publishers*, vol. 6, no. 3, pp. 239–252, Nov. 2003.

[14] R. Ramaswami and K. Sivarajan, *Optical Networks. A Practical Perspective*, Morgan Kaufmann, San Francisco, 2nd edition, 2002.

[15] C. G. Gruber, "Resilient Networks with Non-Simple p-Cycles," in *Proceedings of the International Conference on Telecommunications (ICT)*, (Papeete, Tahiti, French Polynesia), Feb. 2003, vol. 2, pp. 1027–1032.

[16] P. Batchelor, B. van Caenegem, B. Daino, P. Heinzmann, D. R. Hjelme, R. Inkret, H. A. Jäger, M. Joindot, A. Kuchar, E. Le Coquil, P. Leuthold, G. de Marchis, F. Matera, B. Mikac, H. P. Nolting, J. Späth, F. Tillerot, N. Wauters, and C. Weinert, *Ultra High Capacity Optical Transmission Networks*, Faculty of Electrical Engineering and Computing, University of Zagreb, Zagreb, 1999, Final Report of COST Action 239.

[17] R. Hülsermann, S. Bodamer, M. Barry, A. Betker, C. Gauger, M. Jäger, M. Köhn, and J. Späth, "A Set of Typical Transport Network Scenarios for Network Modelling," in *Proceedings of ITG-Fachtagung Photonische Netze*, (Leipzig, Germany), May 2004, pp. 65–72.

[18] R. Inkret, A. Kuchar, and B. Mikac, Eds., *Advanced Infrastructure for Photonic Networks*, Faculty of Electrical Engineering and Computing, University of Zagreb, Zagreb, 2003, Final Report of COST Action 266.

[19] R. Huelsermann and M. Jaeger, "Evaluation of a Shared Backup Approach for Optical Transport Networks," in *Proceedings of the European Conference on Optical Communication (ECOC)*, (Copenhagen, Denmark), Sept. 2002.

[20] K. Zhu and B. Mukherjee, "On-line approaches for provisioning connections of different bandwidth granularities in WDM mesh networks," in *Proceedings of the IEEE/OSA Optical Fiber Communication Conference (OFC)*, (Anaheim, CA, USA), Mar. 2002, pp. 549–551.

[21] ILOG Inc., "CPLEX," `http://www.ilog.com/`, 2003.

[22] W. D. Grover, "The Protected Working Capacity Envelope Concept: An Alternate Paradigm for Automated Service Provisioning," *IEEE Communications Magazine*, vol. 42, no. 1, pp. 62–69, Jan. 2004.

List of Figures

List of Tables